ELSEVIER

Magnetic Resonance Imaging 21 (2003) 745–753

MAGNETIC RESONANCE IMAGING

Fast T2-weighted MR imaging: impact of variation in pulse sequence parameters on image quality and artifacts

Tao Li[a,*], Scott A. Mirowitz[b]

[a]*Department of Radiology University of Maryland Medical Center 22 South Greene Street Baltimore, MD 21201-1595, USA*
[b]*Department of Radiology University of Pittsburgh School of Medicine 200 Lothrop Street Pittsburgh, PA 15213-2582, USA*

Received 2 January 2003; received in revised form 17 April 2003; accepted 18 April 2003

Abstract

The purpose of this study was to quantitatively evaluate in a phantom model the practical impact of alteration of key imaging parameters on image quality and artifacts for the most commonly used fast T_2-weighted MR sequences. These include fast spin-echo (FSE), single shot fast spin-echo (SSFSE), and spin-echo echo-planar imaging (EPI) pulse sequences. We developed a composite phantom with different T1 and T2 values, which was evaluated while stationary as well as during periodic motion. Experiments involved controlled variations in key parameters including effective TE, TR, echo spacing (ESP), receive bandwidth (BW), echo train length (ETL), and shot number (SN). Quantitative analysis consisted of signal-to-noise ratio (SNR), image nonuniformity, full-width-at-half-maximum (i.e., blurring or geometric distortion) and ghosting ratio. Among the fast T_2-weighted sequences, EPI was most sensitive to alterations in imaging parameters. Among imaging parameters that we tested, effective TE, ETL, and shot number most prominently affected image quality and artifacts. Short T_2 objects were more sensitive to alterations in imaging parameters in terms of image quality and artifacts. Optimal clinical application of these fast T_2-weighted imaging pulse sequences requires careful attention to selection of imaging parameters. © 2003 Elsevier Inc. All rights reserved.

Keywords: Magnetic resonance imaging; Magnetic resonance; Rapid imaging; Magnetic resonance; Image quality; Magnetic resonance; Artifact; Phantom study

1. Introduction

Long acquisition time has been a major limitation of T_2-weighted magnetic resonance (MR) imaging, particularly in the evaluation of those organ systems that undergo physiologic motion [1-3]. The recent introduction of enhanced gradient systems and fast pulse sequences has presented new options for body MR imaging. Fast and ultrafast MR imaging sequences introduce the potential for breath-hold or motion-independent imaging, high-resolution imaging, functional imaging, and present the opportunity to consider the feasibility of rapid screening MR examinations [4-6]. To a much greater degree than many other imaging modalities, MR imaging involves a multitude of operating parameter decisions; improper choices can result in impaired image quality and decreased diagnostic efficacy. This may be particularly true where relatively new fast imaging sequences are concerned, since they often involve unfamiliar and complex imaging parameters [7-10].

An understanding of the impact of alterations in imaging parameters on image quality is essential to obtaining optimum clinical results. Although there have been previous investigations regarding the contrast mechanisms and related effects of isolated fast T_2-weighted pulse sequences, there has been no rigorously quantitative analysis of these issues among various sequences. The comparative characterization of imaging parameters and their impacts on image quality and artifact between various pulse sequences are also less addressed. The objective of this study was to quantitatively evaluate in a phantom model the impact of alteration of major imaging parameters on image quality and artifacts for the most commonly used fast T_2-weighted MRI sequences. These include fast spin-echo (FSE), single shot fast spin-echo (SSFSE), and spin-echo echo-planar imaging (EPI) pulse sequences. It is hoped that this study would provide useful guideline for obtaining optimum fast T_2-weighted pulse sequences.

* Corresponding author. Tel.: +1-410-328-7598; fax: +1-410-328-0341.
E-mail address: tli@umm.edu (T. Li).

0730-725X/03/$ – see front matter © 2003 Elsevier Inc. All rights reserved.
doi:10.1016/S0730-725X(03)00173-5

(a)

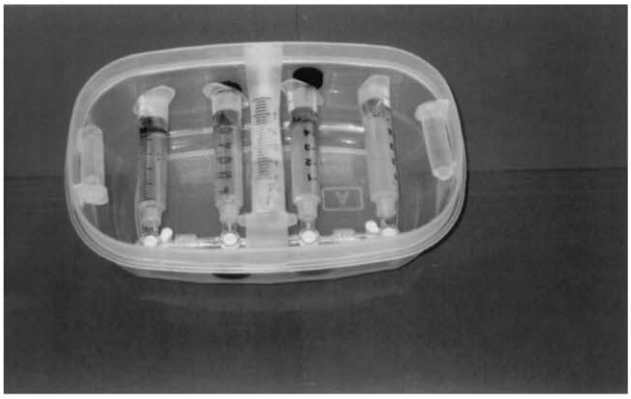

(b)

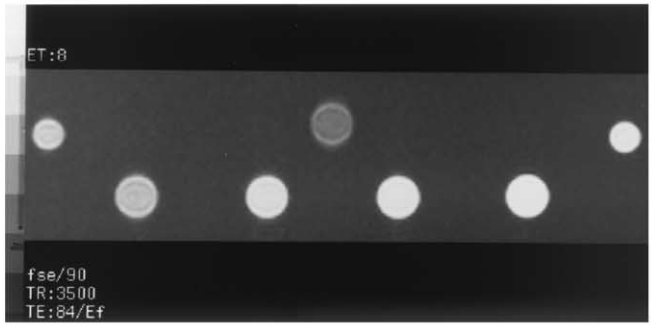

(c)

Fig. 1. MR phantom design. (a) Photograph of the MR compatible ventilator used for moving phantom imaging, (b) Photograph of MR phantom, (c) Axial MR image of phantom.

2. Materials and methods

2.1. Phantom design

We developed a composite phantom consisting of five syringes (12 mm diameter) filled with different concentrations of gadolinium chelate contrast material solution and agarose gel adopted distilled water. These five samples had T2/T1 relaxation times of 37/270, 59/500, 88/960, 182/2500, 307/3500 (msec), respectively, which comprise the range of relaxation values for representative biologic tissues at 1.5 Tesla (Fig. 1). Two additional tubes contained distilled water and vegetable oil, providing references for water and fat.

Several conventional spin echo sequences were acquired in order to calculate T1 and T2 relaxation values for these samples, using the ratio of signal method. These images included T_1-weighted images (TR/TE = 500/20) and proton density-weighted and T_2-weighted images (TR/TE = 2000/20, 80). For this measurement, we applied the following equation to calculate T2: $T2 = (80\text{-}20)/\ln R_2$. A look-up table based on equation $R_1 = (1 - e^{-2000/T1})/(1 - e^{-500/T1})$ was referenced to obtain T1, where R_2 is the ratio of signal intensity at TR/TE = 2000/20 to signal intensity at TR/TE = 2000/80, and R_1 is the ratio of signal intensity at TR/TE = 2000/20 to signal intensity at TR/TE = 500/20.

In order to incorporate the effects of motion, the phantom was subjected to periodic motion with a MR compatible ventilator. This device produced up-and-down motion of 8 mm amplitude at a rate of 16 times/min, in order to simulate respiratory motion.

2.2. Imaging protocols

MR imaging was performed on a Signa 1.5 T system (General Electric Medical Systems, Milwaukee, WI). The fast MR sequences included in this study were those deemed to be in most widespread use for acquisition of fast T_2-weighted MR sequences in current clinical practice. These sequences included FSE, SSFSE, and EPI.

All images were acquired using a 20 × 15 cm field of view (FOV), a 256 (frequency) × 192 (phase) matrix, and one signal average. Three images of 7 mm thickness were acquired with a 1.5 mm intersection gap. Experimental variations in key imaging parameters that were undertaken are described in Tables 1, 2, and 3. The stationary phantom

Table 1
FSE pulse sequence parameters

Protocol	Changed Parameters		Fixed Parameters			
Change of TE	TE(msec)	ES(msec)	TR(msec)	ETL	BW(kHz)	
	14	1.75	3500	16	16	
	50	5.25				
	84	10.5				
	120	15.75				
Change of TR	TR(msec)		TE(msec)	ETL	BW(kHz)	ES(msec)
	2500		84	16	16	10.5
	3500					
	4500					
	5500					
Change of ETL	ETL	ES(msec)	TR(msec)	TE(msec)	BW(kHz)	
	8	21	3500	84	16	
	16	10.5				
	32	5.3				
Change of BW	BW(kHz)		TR(msec)	TE(msec)	ETL	ES(msec)
	16		3500	84	16	10.5
	31					
	62					

was initially imaged and signal-to-noise ratio (SNR), image contrast, homogeneity, blurring, and geometric distortion were measured. Next, the moving phantom was imaged using the same imaging protocols in order to evaluate the effects of motion.

2.3. Quantitative analysis

Quantitative image analysis included measurement of image signal-to-noise ratio (SNR), signal homogeneity (i.e., nonuniformity) and full-width-at-half-maximum (FWHM) (i.e., blurring) in the stationary phantom, and ghosting ratio (GR) in the moving phantom. SNR was calculated as the mean signal intensity of a region-of-interest (ROI) cursor located within the phantom sample, with noise measured as the standard deviation of signal located outside of the phantom sample. Nonuniformity was calculated as the percentage of the standard deviation (SD) of image signal intensity relative to its mean signal intensity (M): nonuniformity = SD/M $\times$ 100% [12]. Thus, higher nonuniformity values indicate reduced signal homogeneity. FWHM was measured on the center phantom section along the phase-encoding direction of the image (Fig. 2). In FSE and SSFSE sequences, FWHM primarily reflects the extent of image blurring. In EPI it also reflects geometric distortion caused by magnetic susceptibility effect. The ghosting ratio (GR) was calculated as the ratio of mean signal intensity of a rectangular ROI positioned outside the phantom sample along the phase-encoding direction to the mean signal intensity of the phantom object (Fig. 3). This is given by the following equation: GR = Gsi/Psi $\times$ 100%, where Gsi is the mean signal intensity of ghost artifact, and Psi is the mean signal intensity of the phantom object. GR measurements were acquired on all three slices for each object, and then averaged to obtain the final result. An identical ROI cursor was used for all measurements. The average change of all phantom objects in NU and GR per unite of TR, TE, BW, ETL and SN was also determined.

Table 2
SSFSE pulse sequence parameters

Protocol	Changed Parameters	Fixed Parameters	
Change of TE	TE(msec)	BW(kHz)	TR(msec)
	69	16	infinite
	97		
	186		
Change of BW	BW(kHz)	TE(msec)	TR(msec)
	31	97	infinite
	62		

3. Results

A summary of the change of average NU and GR by per unit of increasing TR, TE, BW, ETL, and SN is showed in Table 4.

Effect of increasing effective TE—SNR decreased with all three pulse sequences as effective TE increased (Fig. 4). Decrease in SNR of short T2 samples was particularly prominent, which resulted in increased contrast. Image nonuniformity increased by 0.03 and 0.12 per msec TE in FSE and SSFSE. There was no recognizable trend regarding nonuniformity with increasing effective TE for EPI sequences. As effective TE increased, the FWHM of the short T2 (59 msec) object decreased from longer value (13 mm) to the value equal to the original phantom diameter (12 mm), consistent with decreased blurring effect (Fig. 5), whereas FWHM of other phantom objects remained stable in FSE. In SSFSE, the FWHM of all objects—except that with very long T2 (307 msec)—decreased with increasing

Table 3
EPI pulse sequence parameters

Protocol	Changed Parameters		Fixed Parameters			
Change of TE	TE(msec)		TR(msec)	SN	BW(kHz)	ES(msec)
	75		2500	16	32	320
	100					
	125					
Change of TR	TR(msec)		TE(msec)	Shot	BW(kHz)	ES(msec)
	1500		75	16	32	320
	2500					
	3500					
Change of SN	SN	ES(msec)	TR(msec)	TE(msec)	BW(kHz)	
	8	576	2500	75	32	
	16	320				
	32	320				
	48	256				
Change of BW	BW(kHz)	ES(msec)	TR(msec)	TE(msec)	SN	
	16	640	2500	75	16	
	31	320				
	62	320				

TE. This pattern likely reflects signal loss with long TE. In EPI, the FWHM remained stable in nearly all samples, except that with very short T2 (37 msec). In the latter situation, the FWHM increased from 10 to 11 mm as TE increased from 75 to 100 msec. GR increased by 0.07, 0.03 and 0.16 per msec TE in FSE, SSFSE and EPI respectively with increasing effective TE.

Effect of increasing TR—SNR of long T2 objects (182, 307 msec) increased with increasing TR, whereas that of short and medium T2 objects (37, 59, 89 msec) remained relatively stable in both FSE and EPI pulse sequences (Fig. 6). Contrast increased slightly between long T2 and short/medium T2 objects, though no change was noted relative to medium vs. short T2 objects. Image nonuniformity was not

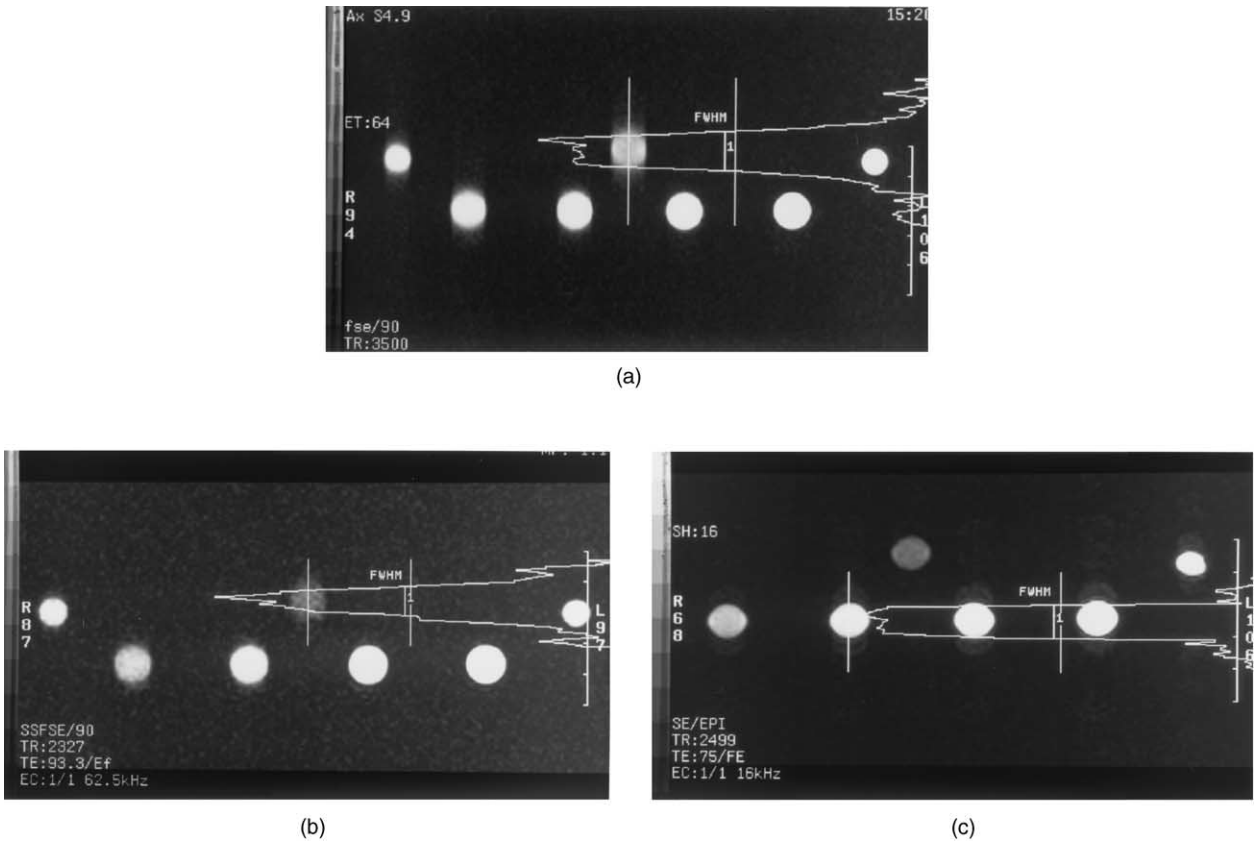

Fig. 2. Measurement of FWHM. (a) In FSE, FWHM may be increased due to the blurring effect. (b) In SSFSE, FWHM may be decreased due to signal loss. (c) In SE-EPI, FWHM is decreased due to geometric distortion.

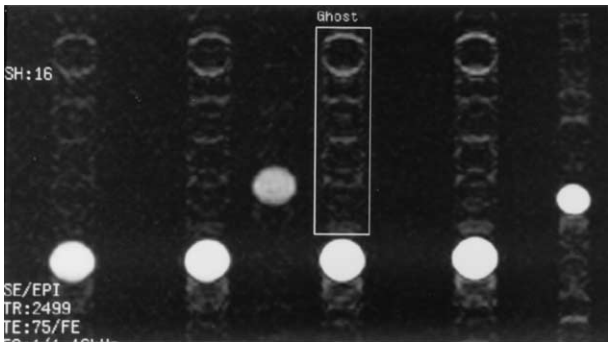

Fig. 3. Measurement of ghost signal intensity.

impacted by alterations in TR on FSE, and there was no recognizable trend in EPI sequences with increasing TR. FWHM in FSE sequences did not change with increasing TR (Fig. 7). In EPI, increased FWHM was observed only at TR 2500 msec where the FWHM of all objects—except that with very short T2 (37 msec)—increased from 10 to 11 mm, indicating reduced geometric distortion. The GR decreased by 1.30 and 1.26 per hundred msec TR in FSE and EPI sequences, respectively, with increasing TR.

Effect of increasing ETL or SN—In FSE sequences increasing ETL resulted in increased SNR, though contrast between the various samples was unchanged (Fig. 8). In EPI, SNR decreased with increasing SN between 8 and 32; thereafter, SNR increased between 32 to 64 shots. Contrast was minimal with use of 32 shots (Fig. 8). Otherwise, there was no significant change in contrast as SN was altered. Image nonuniformity increased slightly by 0.07 per ETL in FSE sequences, and decreased by 0.19 per SN in EPI. The FWHM of short T2 objects (37 and 59 msec) increased in FSE and EPI sequences as ETL or SN increased (Fig. 9). The GR remarkably decreased by 0.50 per ETL in FSE, while it increased by 0.08 per SN in EPI.

Effect of increasing BW—SNR and contrast decreased as BW was increased in all three pulse sequences (Fig. 10). With increasing BW, image nonuniformity increased slightly in FSE and SSFSE sequences, whereas it decreased moderately in EPI. FSE images demonstrated no change in FWHM with increasing BW (Fig. 11). In SSFSE sequences, FWHM decreased as BW was increased, indicating signal

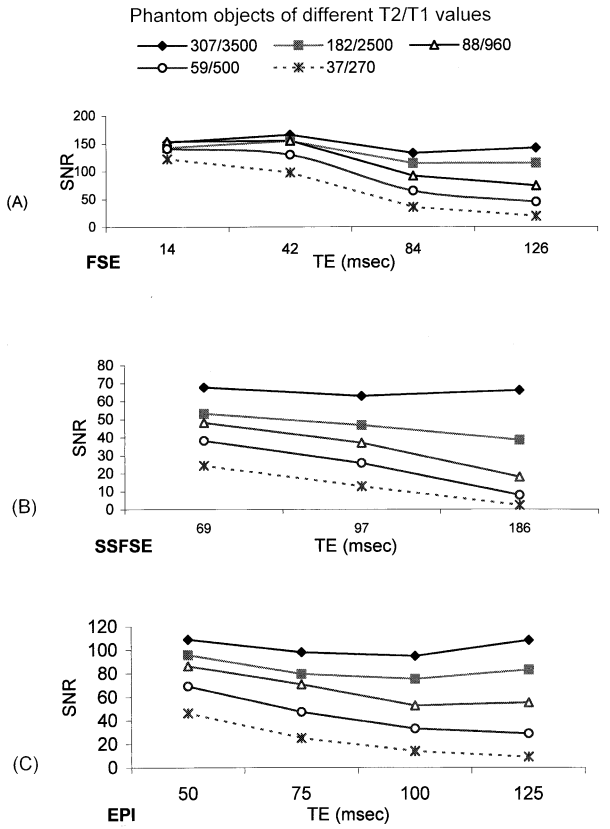

Fig. 4. SNR versus effective TE for FSE (A), SSFSE (B), and EPI (C).

loss. In EPI sequences, FWHM increased with increasing BW, but remained less than the original phantom diameter, indicating reduced geometric distortion. The GR increased slightly FSE sequences, was stable in SSFSE sequences, and increased prominently in EPI sequences as BW was increased.

4. Discussion

T_2-weighted pulse sequences are essential for the detection and characterization of many abnormalities using MR imaging [13]. In conventional spin echo (CSE) images,

Table 4
Change of aNU and aGR by per unit of increasing image parameter

	aNU			aGR		
Increasing Parameters	FSE	SSFSE	EPI	FSE	SSFSE	EPI
Per hundred msec TR	±	N/E	±	−1.30	N/E	−1.26
Per msec TE	0.03	0.12	±	0.07	0.03	0.16
Per kHz BW	0.02	0.05	−0.21	0.05	±	0.19
Per ETL or SN	1.38	N/E	−0.98	−0.50	N/E	0.08

Note: aNU = Average nonuniformity of all 5 phantom objects. aGR = Average ghosting ratio of all 5 phantom objects. BW = Reveive bandwidth. ETL = Echo train length. SN = Shot number. N/E = Not evaluated. ± = No recognizable trend of change. Positive number means increased effect, while negative number means decreased effect.

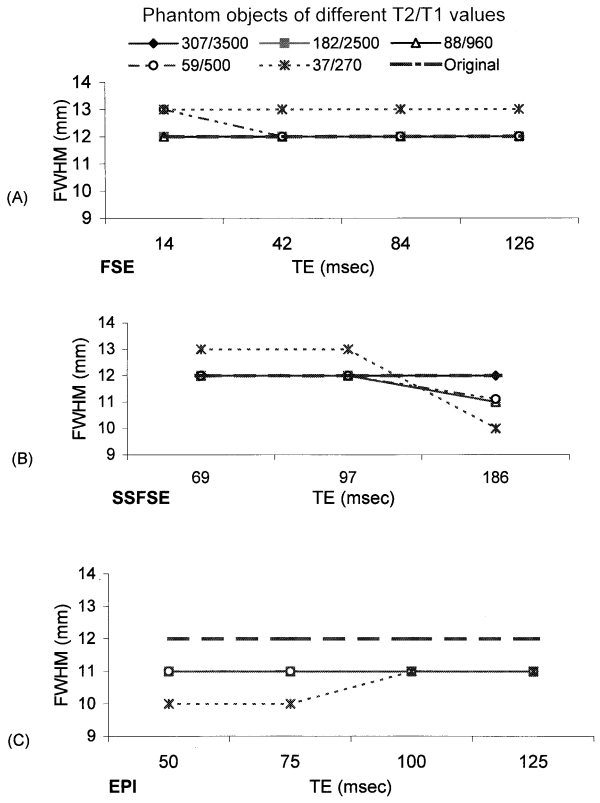

Fig. 5. FWHM versus effective TE for FSE (A), SSFSE (B), and EPI (C).

image degradation related to long acquisition times has been a major limitation in body MR imaging [2,14]. A number of fast imaging techniques have been recently introduced that allow T_2-weighted images to be obtained quite rapidly [5,11,15,16]. FSE, SSFSE and EPI are currently among the

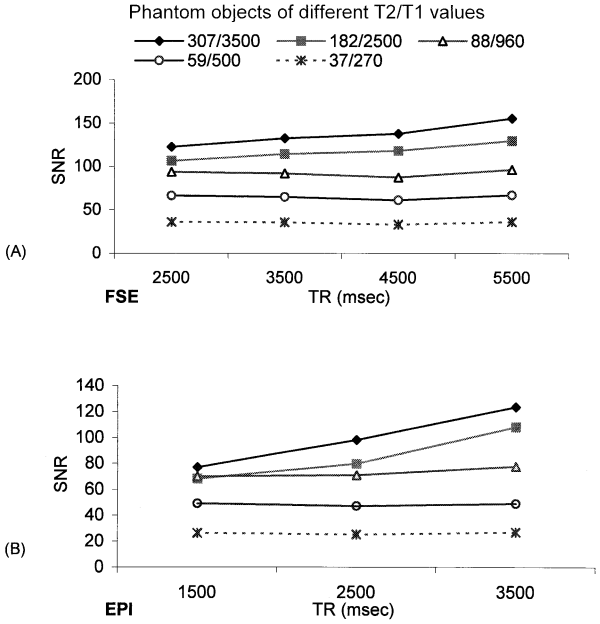

Fig. 6. SNR versus TR for FSE (A) and EPI (B).

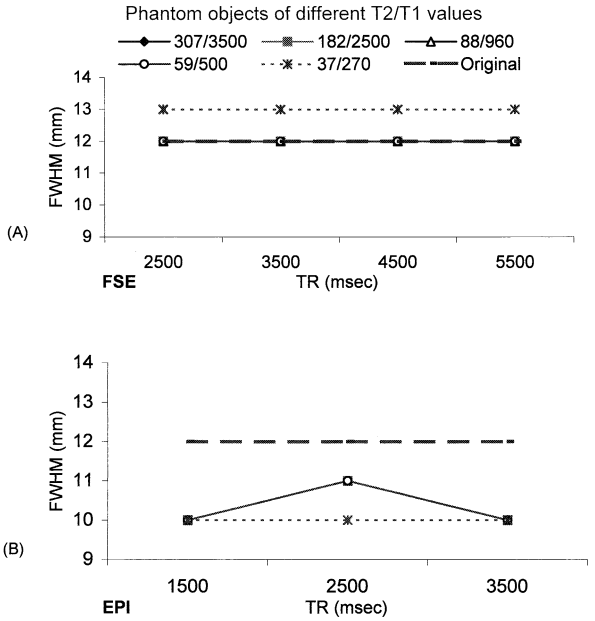

Fig. 7. FWHM versus TR for FSE (A) and EPI (B).

most frequently utilized fast T_2-weighted MR pulse sequences in the clinical setting [5,17,18]. Unlike CSE imaging, in which a single phase-encoding step is acquired per TR, these fast sequences generate multiple phase-encoding steps per TR. Thus, more efficient k-space data filling dramatically reduces image acquisition time [19].

With the introduction of these pulse sequences, optimi-

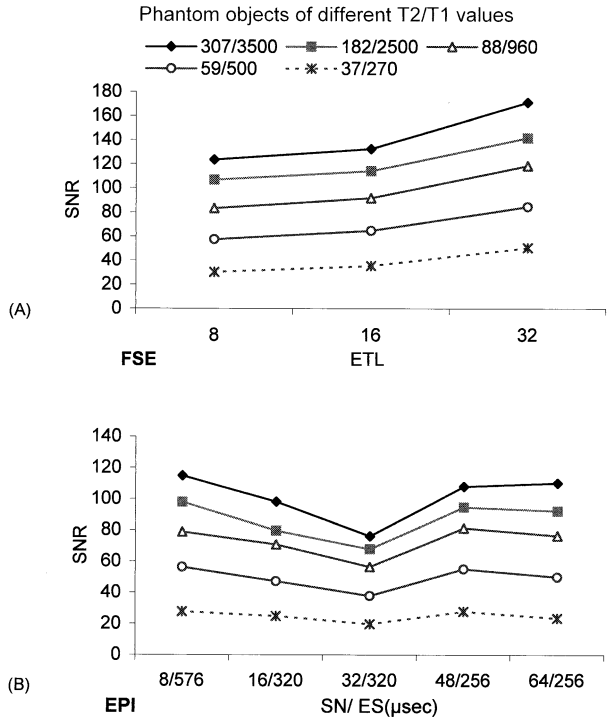

Fig. 8. SNR versus ETL (echo train length) or SN (shot number) for FSE (A) and EPI (B).

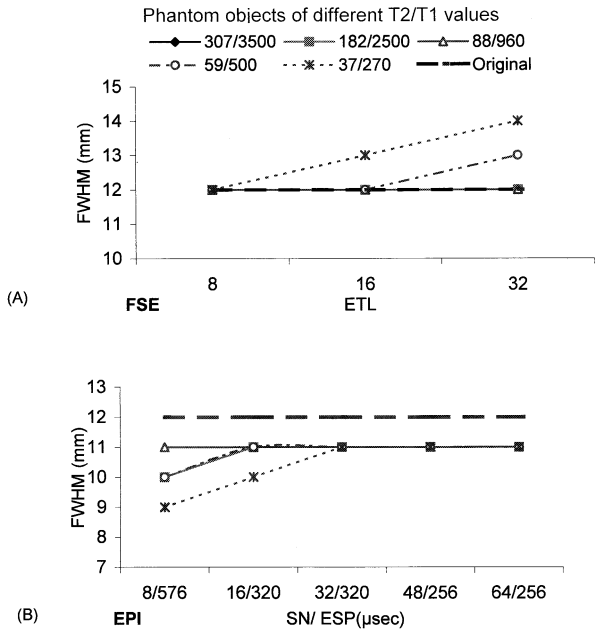

Fig. 9. FWHM versus ETL (echo train length) or SN (shot number) for FSE (A) or EPI (B).

zation of several new imaging parameters must be considered. For example, one must consider the potential impact of sequence parameters such as effective TE, echo spacing, ETL, and SN on image quality [10,19]. In addition, standard

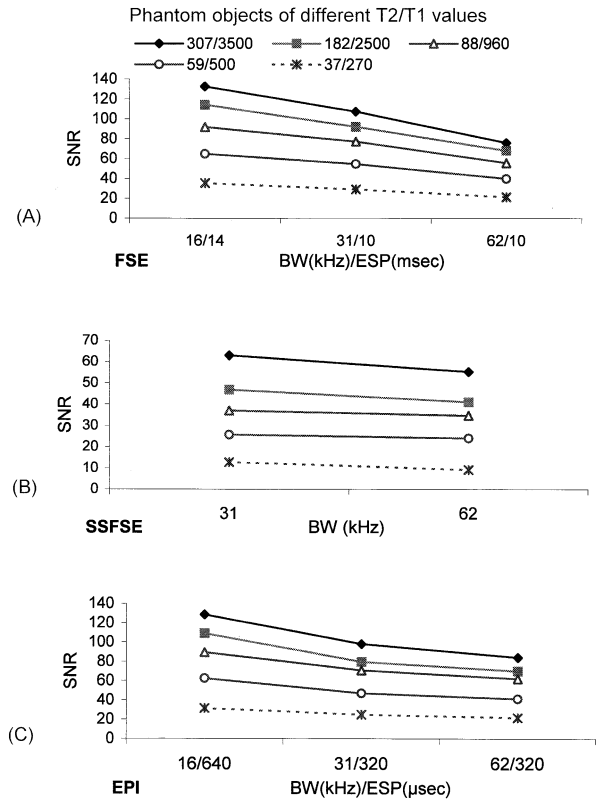

Fig. 10. SNR versus BW for FSE (A), SSFSE (B), and EPI (C).

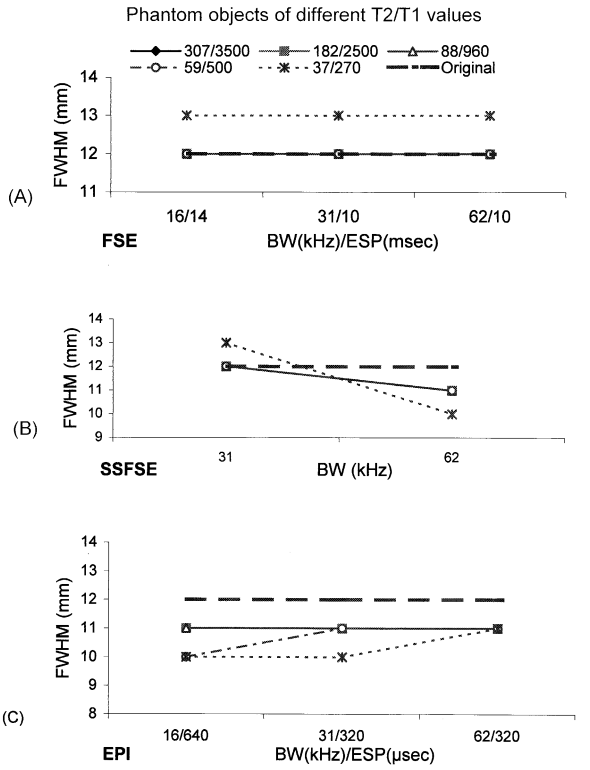

Fig. 11. FWHM versus BW for FSE (A), SSFSE (B), and EPI (C).

imaging parameters such as BW and acquisition matrix can also affect the resultant image differently than in conventional techniques [20]. Furthermore, same imaging parameter may have different effect on image quality between different pulse sequences. In this study, we have quantitatively analyzed the impact of changes in the above imaging parameters on image quality and artifacts in fast T_2-weighted MR imaging, focused on comparative characterization of various imaging parameters and their impacts among these fast pulse sequences, in order to provide general guideline for optimizing T_2-weighted images among various fast pulse sequences.

Altering effective TE had prominent effects in all of the fast T_2-weighted imaging sequences we evaluated. As TE was increased, SNR—especially for short T2 objects—decreased and T2 contrast improved in all sequences. Our results confirm that reduced SNR is a significant limitation encountered with each of these sequences when prolonged TE is used to promote T2 contrast among short T2 tissues (Fig. 4). Image nonuniformity increased in both FSE and SSFSE images with increased TE, presumably due to accentuated magnetic susceptibility effects with longer TE. In EPI, however, there was no correlation between nonuniformity and TE. This is likely because EPI is inherently highly sensitive to magnetic susceptibility effects, changes in image nonuniformity with alterations in effective TE might not be recognizable.

Increasing effective TE only had an obvious impact on image blurring in the phantom object of short T2 (56 msec),

which showed decreased blurring in FSE (Fig. 5A), whereas the very short T2 (36 msec) object was always positive in blurring. Theoretically, increasing effective TE can reduce blurring effect in FSE, but this effect is not observed in long or very short T2 tissues. The blurring in FSE may be described by an effective point spread function (PSF) which is dependent upon imaging parameters (TE, TR and phase-encoding order) and the T2 value of the tissue under consideration [9]. The degree of blurring caused by the action of PSF is inversely related to T2. The effective PSF in short T2 tissue is considerably broader than that in long T2 tissue. Thus short T2 tissue is particularly susceptible to blurring effect in FSE.

In SSFSE, the remarkable change was observed on longer TE (196 msec) images, where the FWHM of objects with short and medium T2 objects (37, 59 and 88 msec) decreased so that they were less than the original FWHM. This observation is attributed to the severe blurring and very low signal intensity of short T2 tissue that occurs with use of a long TE SSFSE sequence. Our results confirm that it is suboptimal to use heavily T_2-weighted SSFSE images to detect small lesions of short T2 values because of these considerations.

The ghosting ratio increased slightly with increasing effective TE in all sequences. In conventional spin-echo techniques, motion artifact is exacerbated because gradient-induced phase errors are compounded during the time between echoes. Thus motion artifact increases as TE becomes longer. With FSE, SSFSE and EPI, however, the time between echoes (echo spacing) is not affected by changes of effective TE. Thus, it would appear no influence on motion artifact. The slight increase of ghosting ratio in all these sequences might be due to unmatched change of signal intensity between phantom objects and ghosts.

We observed that increasing TR had relatively limited influence on image quality, except the ghosting ratio decreased in FSE and EPI sequences with increasing TR. In CSE imaging, changes in TR changes the separation between ghost images based on the formula: separation (pixels) = TR $\times$ Ny $\times$ NEX/t, where Ny is phase-encoding number, NEX is number of excitations, and t is time of motion [3]. Therefore, increasing TR results in increased separation of ghost artifacts, and overall decreased ghosting artifact. In FSE and EPI imaging, increasing TR had a similar effect on the separation of ghost artifacts [24]. Our results indicates that the use of long TR can be helpful in reducing motion effects in FSE and EPI sequences.

ETL refers to the number of echoes acquired per excitation in FSE sequences. SN indicates the number of TR periods that the sequence is repeated in order to obtain the full complement of image data in EPI sequences. ETL and SN are related parameters, though they have an inverse relation. Therefore, the longer the ETL, the fewer the number of shots. Our findings indicate that SNR increases slightly and contrast remains relatively stable with increasing ETL in FSE. This might be due to less T2* effect as increasing ETL. In theory, as ETL increases in FSE sequences, magnetic susceptibility effect decreases due to decreased dephasing from closely spaced refocusing 180 ° pulses. This leaves little time for spins to dephase as they diffuse through regions of magnetic nonuniformity, thus decreasing T2* effect. In EPI, SNR decreased with increasing SN from 8 to 32, and then increased between 32 and 64 shots. It is interesting to note that both SNR and contrast were minimal at SN/ESP pair of 32/320 (μsec). It is anticipated that this set of parameters would yield unsatisfactory clinical results.

Image nonuniformity increased slightly with increasing ETL in FSE, while in EPI it decreased prominently with increasing SN and decreasing ESP. In FSE, increased image nonuniformity is likely due to the average of more echoes with increasing ETL. In EPI, however, decreasing ESP may be much more critical for increasing image homogeneity because magnetic susceptibility effect can be reduced with use of short ESP. We observed that long SN accompanied by short ESP is especially useful for increasing image homogeneity in EPI due to its inherent sensitivity to magnetic susceptibility effect.

FSE blurring increased prominently with increasing ETL. This is because increasing ETL maximizes T2 attenuation differences throughout the echo train [7]. This is a significant limitation when using long ETL in FSE, especially when short effective TE is used simultaneously. In EPI, geometric distortion decreased prominently with increasing SN between 8 and 32 shots, but remained stable between 32 and 64 shots. This is likely because increasing SN decreases ESP, thereby reducing geometric distortion. Our results confirm that increasing SN is helpful for reducing geometric distortion in EPI, though such distortion cannot be eliminated. The ghosting ratio in FSE images decreased remarkably as increasing ETL because of more even-echo rephasing effect caused by increased number of 180° refocusing pulses. This appears to be the most practical method for reducing motion effect in FSE among the variations that we studied. In EPI, ghosting ratio increased slightly as increasing SN. This is attributed to longer acquisition time.

BW, the rate of analog-to-digital conversion of the MR signal, is also referred to as the sampling rate [25]. Increasing BW causes decreased SNR while also decreasing magnetic susceptibility effect. Our findings showed that SNR and T2 contrast decreased in all fast T_2-weighted sequences as BW was increased. Low SNR with decreased T2 contrast was a clear disadvantage when using wide BW, especially in SSFSE images. In the latter situation, use of a wide BW decreased spatial contrast resolution due to severe signal loss. Image nonuniformity only slightly changed in FSE and SSFSE with increasing BW. Whereas, in EPI, image nonuniformity decreased prominently with increasing BW, presumably because both increased BW and decreased ESP reduce magnetic susceptibility effect and thus image nonuniformity. In SSFSE, FWHM decreased with increasing

BW, with the resultant value being less than the original FWHM when BW increased to 62 kHz. This is attributed to reduced contrast caused by severe signal loss with increasing BW. This result indicates that the use of relatively narrow BW should be preferred in SSFSE. Increasing BW had little influence on ghosting ratio in both FSE and SSFSE sequences, but caused increased ghosting ratio in EPI. Therefore, in EPI one must be cautious when implementing wide BW in the presence of physiologic motion.

5. Summary

Our investigation demonstrates the sometimes profound impact that alterations in key imaging parameters can produce on image quality and artifacts for fast T_2-weighted MR sequences (FSE, SSFSE, and EPI). Increasing TE causes SNR of short T2 objects decreased remarkably in all sequences, blurring effect of short T2 object decreased in FSE, and spatial resolution of short T2 objects decreased in SSFSE. TR has relatively limited influence on image quality, except long TRs are helpful in reducing motion effects in FSE and EPI. Increasing ETL in FSE causes SNR and image nonuniformity increased slightly, blurring effect increased prominently, and ghosting ratio reduced remarkably. Increasing SN in EPI causes image nonuniformity and geometric distortion decreased prominently, and ghosting ratio increased slightly. Increasing BW causes SNR and T2 contrast decreased in all sequences. Low SNR with decreased T2 contrast is a clear disadvantage when using wide BW, especially in SSFSE images. Moreover, increasing BW has more profound impact on EPI, causing image nonuniformity decreased prominently, geometric distortion decreased, and ghosting ratio increased.

Acknowledgments

Support for this work was provided by General Electric Medical Systems.

References

[1] Mirowitz SA. Diagnostic pitfalls and artifacts in abdominal MR imaging: a review. Radiology 1998;208:577–89.
[2] Wood ML, Runge VM, Henkelman RM. Overcoming motion in abdominal MR imaging. Am J Roentgenol 1988;150:513–22.
[3] Arena L, Morehouse HT, Safir J. MR imaging artifacts that simulate disease: how to recognize and eliminate them. Radiographics 1995; 15:1373–94.
[4] Davis CP, McKinnon GC, Debatin JF, von Schulthess GK. Ultrahigh-speed MR imaging. Eur Radiol 1996;6:297–311.
[5] Gaa J, Hatabu H, Jenkins RL, Finn JP, Edelman RR. Liver masses: replacement of conventional T2-weighted spin-echo MR imaging with breath-hold MR imaging. Radiology 1996;200:459–64.
[6] Jaegere TD, Van Hoe L, Van Steenbergen W, et al. Screening applications for MRI in the detection of upper abdominal disease: comparative study of non-contrast-enhanced single-shot MRI and contrast-enhanced helical CT. Eur Radiol 1999;9:853–61.
[7] Sze G, Kawamura Y, Negishi C, et al. Fast spin-echo MR imaging of the cervical spine: influence of echo train length and echo spacing on image contrast and quality. Am J Neuroradiol 1993;14:1203–13.
[8] Constable RT, Anderson AW, Zhong J, Gore JC. Factors influencing contrast in fast spin-echo MR imaging. Magn Reson Imaging 1992; 10:497–511.
[9] Constable RT, Gore JC. The loss of small objects in variable TE imaging: implications for FSE, RARE, and EPI. Magn Reson Med 1992;28:9–24.
[10] Reimer P, Saini S, Hahn PF, Brady TJ, Cohen MS. Clinical application of abdominal echoplanar imaging (EPI): optimization using a retrofitted EPI system. J Comput Assist Tomogr 1994;18:673–9.
[11] Yu BC, Jara H, Vanhoenacker PK, Yucel EK. T2-weighted MR imaging of the liver: optimization of hybrid-RARE sequences. Magn Reson Imaging 1997;15:267–73.
[12] Wicks DA, Barker GJ, Tofts PS. Correction of intensity nonuniformity in MR images of any orientation. Magn Reson Imaging 1993; 11:183–96.
[13] Wittenberg J, Stark DD, Forman BH, et al. Differentiation of hepatic metastases from hepatic hemangiomas and cysts by using MR imaging. Am J Roentgenol 1988;151:79–84.
[14] Axel L, Summers RM, Kressel HY, Charles C. Respiratory effects in two-dimensional Fourier transform MR imaging. Radiology 1986; 160:795–801.
[15] Outwater EK, Mitchell DG, Vinitski S. Abdominal MR imaging: evaluation of a fast spin-echo sequence. Radiology 1994;190:425–9.
[16] Yu JS, Kim KW, Kim YH, Jeong EK, Chien D. Comparison of multishot turbo spin echo and HASTE sequences for T2-weighted MRI of liver lesions. J Magn Reson Imaging 1998;8:1079–84.
[17] Edelman RR, Wielopolski P, Schmitt F. Echo-planar MR imaging. Radiology 1994;192:600–12.
[18] Van Hoe L, Bosmans H, Aerts P, et al. Focal liver lesions: fast T2-weighted MR imaging with half-Fourier rapid acquisition with relaxation enhancement. Radiology 1996;201:817–23.
[19] Listerud J, Einstein S, Outwater E, Kressel HY. First principles of fast spin echo. Magn Reson Q 1992;8:199–244.
[20] Mitchell DG, Outwater EK, Vinitski S. Hybrid RARE: implementations for abdominal MR imaging. J Magn Reson Imaging 1994;4: 109–17.
[21] Coates GG, Borrello JA, McFarland EG, Mirowitz SA, Brown JJ. Hepatic T2-weighted MRI: a prospective comparison of sequences, including breath-hold, half-Fourier turbo spin echo (HASTE). J Magn Reson Imaging 1998;8:642–9.
[22] Butts K, Riederer SJ, Ehman RL, Felmlee JP, Grimm RC. Echo-planar imaging of the liver with a standard MR imaging system. Radiology 1993;189:259–64.
[23] Muller MF, Edelman RR. Echo planar imaging of the abdomen. Top Magn Reson Imaging 1995;7:112–9.
[24] Madore B, Henkelman RM. Motion artifacts in fast spin-echo imaging. J Magn Reson Imaging 1994;4:577–84.
[25] Vinitski S, Griffey R, Fuka M, Matwiyoff N, Prost R. Effect of the sampling rate on magnetic resonance imaging. Magn Reson Med 1987;5:278–85.